Structural and electrical defects in amorphous silicon probed by positrons and electrons

S. Roorda[a)]
FOM-Institute for Atomic and Molecular Physics, Kruislaan 407, NL-1098 SJ Amsterdam, The Netherlands

R. A. Hakvoort and A. van Veen
Interfaculty Reactor Institute, Delft University of Technology, Mekelweg 15, NL-2629 JB Delft, The Netherlands

P. A. Stolk and F. W. Saris
FOM-Institute for Atomic and Molecular Physics, Kruislaan 407, NL-1098 SJ Amsterdam, The Netherlands

(Received 4 May 1992; accepted for publication 3 August 1992)

The structure of pure amorphous Si, prepared by ion implantation, has been investigated by variable-energy positron annihilation spectroscopy (PAS) and lifetime measurements of optically generated free carriers. In general, PAS measurements are thought to be sensitive to vacancy-type defects while the carrier lifetime depends on the density of band-gap states (e.g., dangling bonds). The PAS measurements indicate that the density of positron-trapping defects can be reduced by thermal annealing at 500 °C. Concurrent with the removal of structural defects the density of band gap states is reduced as indicated by an increased photocarrier lifetime by a factor of 10. Some material has been implanted with H^+ and annealed at a low temperature (150 °C). The hydrogen is expected to passivate electrical defects associated with strained and dangling bonds and indeed the photocarrier lifetime is increased in this material. Moreover, the PAS measurements cannot distinguish this material from 500 °C annealed amorphous Si, indicating that (some of) the electrical defects are associated with positron-trapping, and therefore possibly vacancy-type, structural defects. Finally, both methods have been used to detect small amounts of ion irradiation damage in annealed amorphous Si.

I. INTRODUCTION

Both amorphous (*a*-) and crystalline (*c*-) Si may contain structural defects. In *c*-Si, many defects have been identified. Examples are the divacancy and the dislocation loop, which have been identified by spectroscopic and imaging techniques such as electron paramagnetic resonance (EPR) and transmission electron microscopy (TEM), respectively. In *a*-Si, only one defect has been identified (by EPR), namely the dangling bond. This identification, however, is limited in the sense that very little is known about the atomic structure surrounding the dangling bond except that it may vary from site to site (whence the wide range of annealing temperatures).[1] Moreover, because EPR has a limited sensitivity (it can only probe a defect if it involves an unpaired electron), it cannot be excluded that other types of defects exist in *a*-Si.

It has been suggested that not only the electrical but also the structural properties of *a*-Si are dominated by defects.[2] In this view structural relaxation, which is also known as short-range ordering, is thought to be mainly controlled by atomic motion similar to the atomic motion responsible for damage repair in heavily defected *c*-Si. Experimental indications supporting this suggestion were primarily based on calorimetry of radiation damage in *a*-Si;[3] it was found that the kinetics and the temperature dependence of annealing of ion irradiation damage in *a*-Si cannot be distinguished from those of defect annealing in similarly treated *c*-Si. It has been corroborated by Raman spectroscopy of ion damage accumulation in relaxed *a*-Si.[4] More recently, measurements of impurity diffusion and solubility in *a*-Si showed complicated behavior that can be understood very well within the framework of a defect mediated structural relaxation in *a*-Si.[5,6] It is noteworthy that the above results, although based on entirely different experimental techniques, are not only in *qualitative*, but also in *quantitative* agreement.[7] In addition to these indirect probes of defects in *a*-Si, there has recently been reported spectroscopic evidence for the vacancy-Sb complex to be microscopically similar in *a*-Si and *c*-Si.[8]

Positron annihilation spectroscopy (PAS) is a sensitive probe of vacancies and vacancy-type defects in metals and semiconductors.[9] It has been used to study monovacancies[10,11] and divacancies[12,13] in *c*-Si but also to detect vacancy-type defects in amorphous metals and voids in both pure and hydrogenated amorphous Si.[14–16] It should be added here that the behavior of positrons in solids is not fully understood. Nonetheless, useful information can be obtained, especially when PAS is combined with other techniques.

For the work described in this article, PAS has been used to study structural relaxation, radiation damage, and defect passivation in *a*-Si; in addition, lifetime measurements of photogenerated carriers have been performed. The PAS results are consistent with the notion that *a*-Si contains a large variety of vacancy-like defect structures,

[a)]Present address: Département de physique, Université de Montréal, 2900 boul. Edouard-Montpetit C.P. 6128, succursale A, Montréal, Québec, H3C 3J7, Canada.

 0021-8979/92/235145-08$04.00

some of which disappear upon thermal annealing. Although the quantitative analysis of the data is limited, the results appear to be in quantitative agreement with the calorimetry and impurity diffusion measurements. From the hydrogen-induced detrapping of metal impurities in *a*-Si, it has been shown that electrical defects in as-implanted *a*-Si are associated with structural imperfections, possibly vacancy-type defects, controlling diffusion of transition metals.[17] Our present results also indicate that such a correlation exists.

It should be pointed out here that this study concerns *pure* and *void-free* *a*-Si rather than hydrogenated *a*-Si (*a*-Si:H). By using Si^+ ion implantation into high-purity *c*-Si targets, *a*-Si can be prepared in a form free of macroscopic voids or impurities which may occur in *a*-Si made by evaporation or sputter deposition.[18,19] Voids especially can have a large effect on the interaction between positrons and *a*-Si, as has already been shown.[14–16] For a comparative study on positron annihilation in *a*-Si prepared by ion implantation, sputtering, or glow-discharge deposition, see Hakvoort *et al.*[20] The aim of the present study is to investigate (changes in) the atomic structure of *a*-Si. Therefore, we have used pure *a*-Si prepared by ion implantation. Our results on H in *a*-Si are expected to relate to *a*-Si:H only insofar as isolated Si—H bonds in *a*-Si:H are concerned and not to clustered Si—H bonds associated with microvoids and internal surfaces.

II. SAMPLE PREPARATION AND MEASUREMENTS

A. Sample preparation

Amorphous layers of ≈ 1 μm thickness were formed on *c*-Si wafers by $^{28}Si^+$ ion implantation (0.5 and 1 MeV, 5×10^{15} cm^{-2} each). The ion beam was defocused and rastered electrostatically over the sample surface. During the implantations, the temperature of the targets, which were heat sunk to a liquid-nitrogen cooled piece of solid copper, was ≈ -100 °C. The ion current was kept below 25 nA, which results in negligible sample heating during the implantations. Several pieces of 15×15 mm^2 were prepared. One piece was set aside (as-implanted). Most pieces were annealed in vacuum at 500 °C for 1 h (annealed), some of which were subsequently reimplanted with 0.5 MeV $^{28}Si^+$ ions, but this time to much lower doses of 2.5×10^{11}, 2.5×10^{12}, or 2.5×10^{13} cm^{-2} (damaged). Pieces of *c*-Si were also subjected to these low-dose implants and the damage profiles (in *c*-Si) measured by ion scattering and channeling of 2 MeV He^+ ions. During the low-dose implants, the samples were not cooled.

Some *a*-Si samples were implanted with H^+ ions and annealed at 150 °C. One implant was performed using an energy of 50 keV and a dose of 1×10^{17} ions/cm^2. This implant resulted in a hydrogen implantation profile that peaks at a depth of ≈ 0.5 μm, where it reaches a local H concentration of ≈ 7 at. %. In addition, a sample was implanted with 2, 4, and 15 keV H_2^+ ions to a dose of 5×10^{15} cm^{-2}, resulting in a hydrogen profile that is distributed over 0.15 μm in the near-surface region. For the low-energy implant, the peak hydrogen concentration is about 2.5 at. %. The 50 keV hydrogen implanted sample was used for PAS measurements; the depth of the hydrogen profile was chosen to optimize the possible effect of defect passivation by implanted H on the PAS measurements. The low-energy implanted material was used for carrier lifetime measurements; the range of the implanted hydrogen corresponds to the probe depth of the laser light.

The (*ex situ*) thermal anneals at 500 °C were performed in a quartz tube vacuum furnace at a pressure below 10^{-6} mbar; the (*in situ*) thermal anneals at 150 °C in between PAS measurements were performed by heating a filament in close proximity of the sample. The temperatures are nominal values only.

B. Positron spectroscopy

All samples were irradiated (at room temperature) with mono-energetic positrons and the Doppler shape parameter S was determined as a function of the positron energy (E). This parameter is dependent on the width of the gamma ray peak due to annihilation of positrons with electrons. The positron energy ranged from 0.25 to 25 keV. The figures show only the measurements up to $E=15$ keV; higher energy positrons probe at a depth exceeding that where the ion damage is located. The variable energy positron facility has been described elsewhere in detail.[21,22] The width of the gamma-ray annihilation spectrum depends on Doppler broadening effects and reflects the momentum distribution of the electrons with which the positrons annihilate; it is generally expressed as the S (sharpness) parameter, where a large S corresponds to a narrow energy distribution.[9] S has certain characteristic values depending on where annihilation takes place: At the surface, in the perfect solid, or at a defect site in the solid. Annihilation in different kinds of defect sites can also give rise to different S values. The measured S parameter is a weighted average of the different contributions. In order to correct for possible drift (between different sets of measurements) in the electronics used to measure the annihilation spectrum, each set of measurements includes a measurement on *c*-Si and the S parameters are normalized to the S parameter of the bulk of *c*-Si. For a more detailed account of position annihilation and S-parameters, see Schultz and Lynn[9] and van Veen *et al.*[23]

The measured $S(E)$ curves can be described by theoretical fits to the positron diffusion-annihilation equation, which allows the positron diffusion length to be extracted.[9,22,23] Such fits assume certain energy-dependent positron implantation profiles. We have assumed a Makhovian profile with parameters $n=1.6$ and $m=2.0$.[9] For homogeneous materials (that is, without depth-dependent defect profiles), the only free parameters in the fit are the S parameter at the surface and in the bulk and the positron diffusion length L.

C. Carrier lifetimes

In addition to PAS measurements, some of the samples were characterized by lifetime measurements of optically generated free carriers. Electron-hole plasmas in *a*-Si were

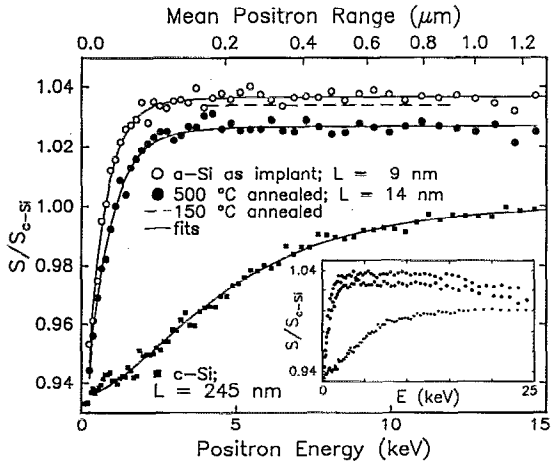

FIG. 1. S parameter (normalized to bulk c-Si) as a function of positron implantation energy for c-Si (squares), and for as-implanted (solid circles) and 500 °C annealed (open circles) pure a-Si. The depth scale (top) corresponds to the mean positron range. Solid lines indicate fits to the data. Dashed line indicates S_b value of 150 °C annealed a-Si. The inset shows the same data over the whole positron energy range.

generated and probed using pulses from a colliding pulse mode-locked laser (CPM).[24] The 100 fs duration pulses of 0.1 nJ each have an average wavelength of 620 nm and are produced at a repetition rate of 110 MHz. The output of the CPM was split into two beams, the first (pump) was chopped at 50 kHz and focused to a 25 μm spot, yielding an energy density of $\approx 4\ \mu J/cm^2$. The second (probe) was sent through a mechanical delay line and focused to a 15 μm spot. The energy density in the probe spot was about one tenth of that in the pump. The probe and a sample of the pump were detected by photodiodes. Using a lock-in technique, the observable relative reflectivity change is $\approx 2\times 10^{-6}$. The experimental setup has been described in more detail elsewhere.[25,26]

III. RESULTS

A. Ion implantation amorphized a-Si and thermal annealing

In Fig. 1, the positron annihilation radiation Doppler broadening parameter S is shown as a function of the positron implantation energy E [i.e., $S(E)$] for c-Si, as-implanted a-Si, and annealed a-Si. The top axis shows the mean depth z of the positrons, with z proportional to $E^{1.6}$ (see Schultz and Lynn[9]). $S(E)$ for c-Si is similar to earlier measurements on the same system and can be interpreted as follows. For very low positron energies, a large fraction of the annihilation events takes place at the surface (i.e., on or in the native oxide) and this is accompanied by a low surface S (S_s) value of 0.92. For high positron energies (>15 keV, shown in inset), all annihilation takes place in the undamaged crystal and this gives the S value of defect-free c-Si $S_{c\text{-Si}} \equiv 1.0000$. For intermediate energies, some positrons annihilate at the surface and some in the bulk, therefore S is a weighted average of S_s and $S_{c\text{-Si}}$. The slope of $S(E)$ is related to the diffusion length L of the positrons in c-Si, which turns out to be 245 nm in this sample, in good agreement with literature.[27,28] This value is the result of fitting the data to the positron diffusion/annihilation equation.[23] All resulting parameters L and S_b are listed in Table I (the values in the table are averaged over several samples and may differ slightly from those shown in the figures).

The $S(E)$ measurements for the a-Si samples differ in two ways from that for c-Si: (1) The bulk value S_b is considerably higher, and (2): the slope with which this value is approached is much steeper in a-Si than in c-Si. Both effects are in accordance with the results of Hautojärvi *et al.*[29] and Nielsen.[30] The values of L and S_b for a-Si in the as-implanted state are 9 nm and 1.0379, respectively. It is now observed that annealing at 500 °C results in a slight decrease of S_b (to 1.0257) and a substantial increase in L (to 14 nm). It should be noted that such a temperature is far below that necessary for noticeable crystal nucleation[31] while solid phase epitaxial crystallization at the c-Si/a-Si interface is limited to a few angströms.[32] Annealing of as-implanted a-Si at a still lower temperature of 150 °C led to small but noticeable changes in the $S(E)$ curve. These data are not shown here except for the dashed line indicating the level of S_b, but the results of curve fitting are reported in Table I.

It is believed that a-Si contains a wide variety of structural imperfections, including vacancy-type defects.[3–6] These defects are expected to act as traps for positrons, thus reducing the diffusion length and increasing S. A detailed discussion and analysis of these data in terms of positron trapping at defects can be found in Sec. IV.

TABLE I. Results of positron diffusion and annihilation fitting (S_b,L) and carrier lifetime measurements (τ).

Sample description	2nd implant	Anneal temp. (°C)	S_b ($\pm 3\times 10^{-4}$)	L(nm) (± 0.5)	τ(ps) ($\pm 10\%$)
c-Si	···	···	1.0000	245±5	···
As-implanted	···	···	1.0379	8.6	1
Low T annealed	···	150	1.0336	···	1.6
High T annealed	···	500	1.0257	15.5	11
Deep hydrogen	50 keV H^+	150	1.0249	···	···
Shallow hydrogen	2,4,15 keV H_2^+	150	···	···	1.6&13
Damaged (0.5 MeV Si^+)	2.5×10^{11} cm^{-2}	(500)	1.0308	16.3	···
Damaged (0.5 MeV Si^+)	2.5×10^{12} cm^{-2}	(500)	1.0317	15.0	···
Damaged (0.5 MeV Si^+)	2.5×10^{13} cm^{-2}	(500)	1.0369	13.7	···

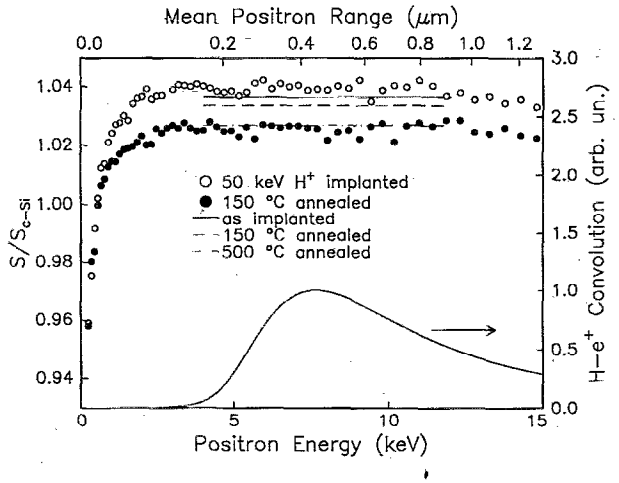

FIG. 2. S parameter (normalized to bulk c-Si) as a function of positron implantation energy for a-Si co-implanted with hydrogen (open circles), and after prolonged annealing at 150 °C (solid circles). The values for S_b of pure a-Si (as-implanted and after 150 or 500 °C anneals) shown in Fig. 1 are indicated. The depth scale (top) corresponds to the mean positron range. In addition, the overlap of the positron implantation profile with the estimated hydrogen implantation depth profile is shown (bottom curve).

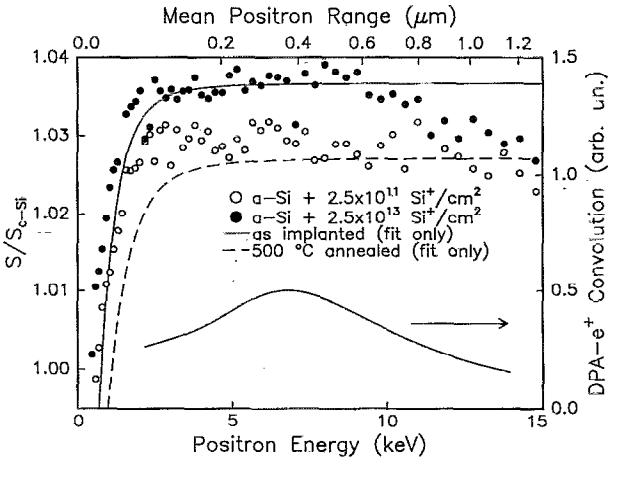

FIG. 3. S parameter (normalized to bulk c-Si) as a function of positron implantation energy for a-Si annealed at 500 °C and then implanted with 500 keV Si^+ ions to a dose of 2.5×10^{11} cm^{-2} (open circles) and 2.5×10^{13} cm^{-2} (solid circles). The fits to the data for as-implanted and 500 °C annealed a-Si shown in Fig. 1 are reproduced. The depth scale (top) corresponds to the mean positron range. The overlap of the positron implantation profile with the estimated ion damage depth profile is also shown (bottom curve).

B. Hydrogen implantation and annealing

In this section we describe the measurements on a-Si that was co-implanted with H^+ ions. It should be noted that this material is not grown like conventional hydrogenated a-Si (a-Si:H) and therefore may have different properties. The absence of macroscopic voids in ion-implanted a-Si, for example, may preclude the presence of clustered H that is normally found in a-Si:H. Figure 2 shows the $S(E)$ curves taken on a-Si that had been co-implanted with 50 keV, 5×10^{16} cm^{-2} H^+. The points for material that has not been annealed are shown as open circles; solid circles represent material that had been annealed *in situ* at $\approx$150 °C for 25 h. The lines indicate the values of S_b for as-implanted, 150 °C annealed, and 500 °C annealed a-Si (without hydrogen) taken from Fig. 1. In addition, the depth profile of the implanted hydrogen, according to calculation and convoluted with the positron implantation profile, is shown as a solid line in the bottom of the figure.

It can be seen in Fig. 2 that merely implanting hydrogen does not change the interaction of positrons with the a-Si to a measurable extent, except perhaps a small increase in S_b. However, the anneal behavior of this material differs from that of pure a-Si. This is evident from the change in S_b, which reaches a value equal to that in 500 °C annealed pure a-Si after prolonged (25 h) annealing at 150 °C. Unfortunately, it is not possible to extract useful values for S_b and L from the data shown in Fig. 2. The diffusion length is determined from the $S(E)$ behavior close to the surface; comparison with the convoluted hydrogen implantation profile (bottom curve) shows that no hydrogen is expected in that region. Nonetheless, it appears that the effect of high-temperature annealing of pure a-Si on the PAS measurements (decreasing S_b) can be mimicked by hydrogen implantation and low-temperature annealing. It is well known that hydrogen passivates electrical defects in a-Si; the present result therefore suggests a connection between the passivation of dangling and strained bonds by H and the high temperature anneal behavior of pure a-Si, a connection that will be discussed in more detail in Sec. IV.

C. Radiation damage in annealed a-Si

In the previous two sections, the effect of thermal annealing on the interaction between positrons and a-Si has been investigated. This section deals with data on the inverse effect: Positrons have been used to detect the damage generated in *annealed* a-Si by ion bombardment. Three samples of a-Si were prepared by ion implantation as described in Sec. II and annealed in vacuum at 500 °C. Following the anneal treatment, the specimens were bombarded with 500 keV Si^+ ions to a dose of 2.5×10^{11}, 2.5×10^{12}, and 2.5×10^{13} cm^{-2}, respectively. The depth profile of displaced target atoms due to violent nuclear collisions (in displacements per atom, DPA) was estimated using Monte Carlo simulation.[33] The amount of ion damage in the a-Si samples has also been estimated by channeling measurements of 2 MeV He^+ ions backscattered from identically bombarded c-Si samples. A piece of c-Si bombarded with 2.5×10^{11} Si^+ ions/cm^2 could not be distinguished from unimplanted c-Si, indicating that the density of displaced atoms is well below an at. %. The other samples did show a measurable increase in the dechanneling. The dechanneled yield in the sample bombarded with 2.5×10^{12} Si^+/cm^2 was consistent with 0.013 DPA and the yield in the 2.5×10^{13} Si^+/cm^2 sample was indicative of $>$ 0.10 DPA. The $S(E)$ curves for two of the ion damaged a-Si samples (2.5×10^{11} and 2.5×10^{13} cm^{-2}) are shown in Fig. 3 as open circles and solid circles. The data for the

2.5×10^{12} cm^{-2} sample is not shown but is intermediate between the other two datasets. The fits to the data for as-implanted and 500 °C annealed a-Si are reproduced from Fig. 1 for comparison (lines). In addition, the solid curve in the bottom of the figure shows the convolution of the positron implantation profile with the calculated ion damage profile; it shows that the effect of ion damage on the $S(E)$ curves will be most pronounced for positron energies between 4 and 10 keV.

The $S(E)$ curve for a-Si bombarded with the lowest ion dose already differs from that of annealed a-Si. For annealed a-Si, bombarded with 500 keV Si^+ ions to a dose of 2.5×10^{11} cm^{-2}, the density of displaced Si atoms (according to Monte Carlo simulation) is at most 2×10^{-4}. Moreover, the ion channeling measurements on the c-Si samples suggest that the density of displaced target atoms is as low as 0.001 DPA. Yet the PAS measurements clearly distinguish between this slightly damaged annealed a-Si, and annealed a-Si that had not been reimplanted. It shows that PAS is a sensitive technique for detection of displacement damage in a-Si.

The $S(E)$ curve for annealed a-Si, bombarded with 2.5×10^{13} Si^+ ions/cm^2 already closely resembles the curve for a-Si in the as-implanted state. Apparently the damage generated by ion bombardment begins to saturate when the density of displaced target atoms is several at. %. Another possible explanation could be that the saturation occurs not in the defect concentration itself but in the trapping of positrons. A saturation has also been observed by Raman spectroscopy measurements[3] and calorimetry[4] of ion damage in a-Si. It suggests that the defect density in a-Si cannot exceed a few at. %.

The visual inspection of Fig. 3 can be aided by using the same fitting procedure as has been used in Fig. 1. The first 7 keV of the positron energy range of all three $S(E)$ curves shown in Fig. 3 have been fitted and the results are displayed in Table I. (These fits assume a homogeneous damage profile and serve as estimates of average values for S_b and L; extraction of damage profiles has not been attempted.) The same differences discussed above can be seen in the table. First, there is already a marked difference between S_b of 500 °C annealed a-Si (1.0257) and that of the least damaged sample (1.0308). Second, the value for S_b in the most highly damaged a-Si (1.0396) is close to that of as-implanted a-Si (1.0379), indicating saturation. In addition, the effective diffusion length is seen to decrease with increasing damage dose.

D. Carrier lifetime measurements

The damage annealing, passivation, and generation in a-Si having been characterized by positrons, we turn to characterization with electrons. Free carriers (electrons and holes) have been generated and detected optically in samples similar to those previously investigated with positrons. Measurements of the reflectivity as a function of time, following generation of a plasma of free carriers by a 100 fs light pulse, are shown in Fig. 4. Four measurements are shown; (a) as-implanted a-Si, (b) a-Si annealed in vacuum at 500 °C, (c) a-Si co-implanted with low-energy H^+ and annealed at 150 °C, and (d) a-Si annealed at 500 °C and then bombarded with 1 MeV Si^+ ions to a dose of 2×10^{13} cm^{-2}. The data are shown as points while the lines represent fits assuming a single exponential decay of the photogenerated plasma and a time resolution of 0.2 ps. One exception is the line shown in Fig. 4(c), which will be discussed below.

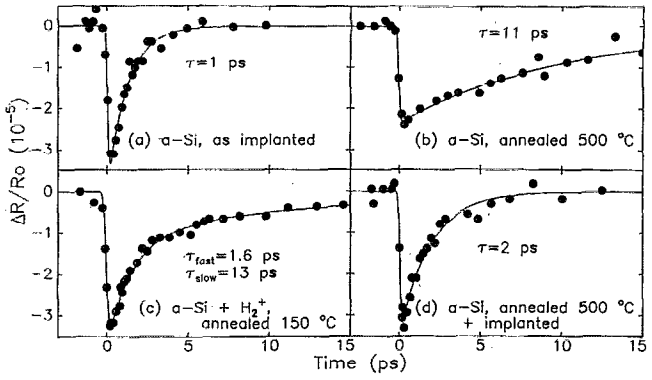

FIG. 4. Normalized reflectivity changes (points) as a function of time difference between pump and probe for (a) as-implanted a-Si, (b) a-Si annealed in vacuum at 500 °C, (c) a-Si co-implanted with low-energy H^+ and annealed at 150 °C, and (d) a-Si annealed at 500 °C and reimplanted with 1 MeV Si^+ ions to a dose of 3×10^{-3} DPA. Time 0 corresponds to overlap of pump and probe. Solid lines are exponential decay curves convoluted with the experimental resolution.

For as-implanted a-Si [Fig. 1(a)], the reflectivity returns to its original level within several picoseconds. The reflectivity for 500 °C annealed a-Si recovers significantly slower, and only after 60 ps the initial reflectivity is reached (not shown). A significant positive change in reflectivity, which would be indicative of sample heating,[34,35] has not been observed at the low laser intensities employed for these measurements. Higher irradiation conditions would also lead to a situation where Auger recombination processes become important.[34,36] The decay time τ, deduced from the single exponential decay curves shown as lines, is 1 ps in as-implanted a-Si, and 11 ps in a-Si, which had been annealed at 500 °C.

The sample that had been co-implanted with low-energy H^+ and annealed at 150 °C shows a reflectivity recovery, shown in Fig. 4(c), intermediate between those of the previous two samples. The reflectivity initially decays at the same rate as that measured for pure a-Si, annealed at 150 °C ($\tau=1.6$ ps), but is followed by a significantly slower process ($\tau=13$ ps). In our opinion, this is caused by the light probing two distinct regions. Around the hydrogen peak in the profile at ≈0.1 μm, electrical defects have been passivated but deeper (and shallower) layers that are also probed have not changed at all, except for a small thermal effect resulting from the 150 °C anneal ($\tau=1.6$ ps). The line through the datapoints represents the sum of two single exponential decay curves with $\tau=1.6$ and 13 ps and relative intensities 70% and 30%, respectively.

An a-Si sample that had been annealed at 500 °C and subsequently reimplanted with 1 MeV Si^+ ions to a dose of 2×10^{13} cm^{-2} has also been measured and the results are

shown in Fig. 4(d). The density of displaced target atoms in the near-surface layer of this sample has been estimated[33] to amount to 0.3 at. %. The reflectivity is observed to return quickly to its original value. Similar to the reflectivity decay curves of as-implanted and 500 °C annealed *a*-Si, it can be characterized by a single exponential decay time but with a value of $\tau=2$ ps. It appears that photocarrier lifetime measurements, like PAS, can be used as a sensitive probe of collisional damage in annealed *a*-Si. A full report of lifetime measurements in *a*-Si and *c*-Si, including ion dose and projectile mass dependence will be given elsewhere.[26,37]

IV. DISCUSSION

A. Positron trapping at defects, qualitative

1. Networks and defects

The most obvious explanation of the present PAS data is in terms of structural defects acting as traps for the positrons. Starting from a (hypothetical) defect-free continuous random network (CRN), real *a*-Si can be represented as a CRN with defects. These defects can be unique to the network (e.g., single dangling or floating bonds) or may be similar to point defects and small point defect clusters in *c*-Si (e.g., divacancies). In principle, both vacancy and interstitial-type defects may exist in *a*-Si, but positron trapping is most likely to occur only at vacancy-type defects.

Structural defects in *a*-Si are expected to be accompanied by a strain field, similar to that surrounding point defects in *c*-Si. Differences in the defect population in the *a*-Si network are then thought to give rise to the variable short-range-order or structural relaxation phenomena. In addition, it is reasonable to expect that structural defects have dangling or highly strained bonds (or both) associated with them. These would give rise to band-gap states that are not necessarily unique for the CRN but similar to defect states in *c*-Si.

Structural defects can be removed by thermal annealing, they can be generated by ion irradiation, and the electrical activity can be passivated by hydrogen. Such treatments are expected to modify the interaction of positrons with *a*-Si because vacancy-type defects are known to act as traps for positrons. A high concentration of defects therefore reduces the positron diffusion length. Annealing or passivation is expected to lead to larger, and ion irradiation to smaller diffusion lengths. This is exactly what is observed in the Figs. 1 and 3. In addition to changes in the positron diffusion length, changes in the bulk S parameter are observed.

The S parameter reflects the momentum distribution of the electrons with which the positrons annihilate. When a distribution of defects is present, the observed S parameter is the weighted average of the S parameter in the bulk and that characteristic of each of the defects

$$S=\left(f_b S_b+\sum_{i=0}^{n} f_i S_i\right)\Big/\left(f_b+\sum_{i=0}^{n} f_i\right), \qquad (1)$$

where f_b is the fraction of positrons annihilating in a defect-free region yielding S_b as S parameter, f_0 is the fraction of positrons annihilating from a surface or parapositronium state, yielding S_0 as effective S parameter, while f_i $(i=1,...,n)$ represents the fraction of positrons annihilating in the ith type of defect, each with its characteristic S parameter S_i (note: $f_b+\Sigma_{i=0}^{n} f_i=1$). From the values of L (see Table I) and based on the assumption that the positron diffusivity in *a*-Si equals that in *c*-Si, it appears that the vast majority of the positrons are trapped. The fact that S changes upon annealing would indicate that the distribution of defects changes; some defect species anneal out but others remain.

2. Other interpretations

Other interpretations of the PAS data are possible, some of which cannot be completely excluded. The slope in $S(E)$ may not be due solely to positron diffusion but to positron drift in an electric field (band bending) that might be present near the surface. Although in *a*-Si such a field is not expected to penetrate far into the material (because of the high density of states in the gap), it may play a role in the case of *c*-Si. This would make it hard to quantify the present results (see next section) but the qualitative conclusion that the trapping rate in *a*-Si reduces upon annealing would still be valid. Changes in S could also be due to a change in density, especially in a covalently bonded material. However, it has been shown that although the density of *a*-Si prepared by ion implantation is 1.7% less than that of *c*-Si, it does not change more than 0.1% by thermal annealing up to temperatures of 580 °C.[38,39] Such a density change is far too small to cause the changes observed in S. Moreover, upon annealing *a*-Si expands rather than compacts,[39] which would give rise to an increase in S rather than a decrease.

An alternative scenario to explain both the change in S and in L induced by thermal annealing of *a*-Si could be that the same number of defects are present, but that the character of (some of) the defects changes. If, for example, some of the defects assume a positive charge state, positrons will be repelled and the trapping rate for that particular defect strongly reduced. In this context, it should be remarked that free-carrier capture is to some extent analogous to the capture of positrons at defect centers.[40] A reduction in the density of trapping (or recombination) centers has been observed by carrier lifetime measurements (see Fig. 4), where the negatively charged electron is thought to be the main probe (the hole mobility is much smaller than that of the electron). When both negatively and positively charged probes experience a reduced decay rate, the most likely explanation is an actual reduction in the number of trapping sites.

B. Positron trapping at defects, quantitative

In this section, we will try to obtain a quantitative estimate of the defect concentrations in the samples studied. Such an estimate requires knowledge of both the diffusivity of positrons in defect-free *a*-Si and the cross section

for positron trapping at each of the possible defects (in every possible charge state). Neither is known and therefore we have to make some assumptions about these quantities, namely that they are equal (or at least similar) to the corresponding properties in *c*-Si. It is pointed out that the mechanisms by which positrons diffuse and are trapped in *c*-Si are not at present fully understood. Therefore, the assumptions have to be taken with some reserve.

The positron diffusivity in *c*-Si has been measured by Nielsen *et al.*[27] and by Schultz *et al.*[28] The diffusivity at room temperature is about 2.7 cm^2/s. Positron trapping rates at defects are largely unknown, but some values have been reported for the neutral divacancy in *c*-Si. Calculations of trapping rates at single vacancies or multivacancy complexes have shown that the trapping rate does not depend very strongly on the size of the defect.[40,41] Therefore, we will use the divacancy trapping rate as a typical positron trapping rate ν in damaged Si. Experimental values for the specific trapping rate at the divacancy are on the order of $\nu=3\times10^{14}\ s^{-1}$.[41–43]

The concentration C of positron traps can be estimated from a comparison of the positron diffusion lengths L in *c*-Si and in *a*-Si using two simple relations between L, D, ν, and C. The diffusion length L is related to the diffusivity D and the effective positron trapping rate λ_{eff} (the inverse of the time before trapping or annihilation) as

$$L=\sqrt{D/\lambda_{\text{eff}}}. \tag{2}$$

The effective positron trapping rate λ_{eff} is related to ν and C according to

$$\lambda_{\text{eff}}=\lambda_b+\nu C, \tag{3}$$

where λ_b is the annihilation rate (inverse positron lifetime) in trap-free *a*-Si (assumed to be equal to that in *c*-Si). Under these relations and assumptions, and using the above values for positron diffusivity and trapping, the trap density in as-implanted *a*-Si would correspond to 1.2 at. %. The defect density in 500 °C annealed *a*-Si is then found to be 0.4 at. %. These numbers give us some faith in the validity of the assumptions because they are in good agreement with estimates based on entirely different methods, namely calorimetry, Raman spectroscopy combined with Monte Carlo damage calculations,[7] and impurity diffusion measurements.[6]

The estimated defect densities in as-implanted and 500 °C annealed *a*-Si are consistent with the PAS measurements on annealed and reimplanted *a*-Si. The minimum amount of ion damage that could be distinguished was on the order of 10^{-3} DPA while the damage had saturated at DPA values of several at. %.

C. Structural and electrical defects

Positrons are known to probe vacancy-like defects in both crystalline and amorphous metals and in crystalline semiconductors. It is not unreasonable, therefore, to expect that positrons probe vacancy-type defects in amorphous Si. In the previous paragraphs it has been argued that the results shown in Fig. 1 are indicative of a thermally induced removal of vacancy-type defects in *a*-Si. The photocarrier lifetime measurements [Figs. 4(a) and 4(b)] show that concurrent with the removal of vacancy-type defects, the number of band-gap states (e.g., dangling bonds) is sharply reduced. This already suggests that a correlation exists between structural and electrical defects in *a*-Si.

The existence of such a relation is corroborated by the results on hydrogen-implanted *a*-Si. Implantation of hydrogen and thermal annealing at 150 °C leads to a reduced number of band-gap states as evidenced by the relatively long photocarrier lifetime in that material [see Fig. 4(c)]. That result was not unexpected because it has long been known that hydrogen passivates dangling bonds, thereby reducing the number of band-gap states. The PAS measurements on hydrogen implanted and 150 °C annealed *a*-Si indicate that the trapping of positrons is also affected. In that case, the anneal temperature is too low for any significant structural changes to occur. It appears, therefore, that some of the vacancy-type defects that were able to trap positrons no longer serve as such traps after the dangling bonds have been passivated with hydrogen. This suggests that (some of) the hydrogen atoms are now occupying the vacancies, which in turn means that (at least some of) the original dangling bonds were located at vacancy-type defects.

Although it is fully expected that the formation and removal of vacancy-type defects leads to the appearance and disappearance of dangling bonds, it is not easily shown experimentally. A spatial relation between defective bonds and radiation damage sites in ion-bombarded *a*-Si has previously been suggested to exist by Heidemann *et al.*,[44] who used ellipsometry of bevelled *a*-Si samples. Moreover, Coffa *et al.*[17] observed that hydrogen implanted in *a*-Si leads to detrapping of metal impurities that had previously been gettered in a defected *a*-Si layer. This strongly suggests that the electrical defects are located at the same site as the structural defects that can trap metal atoms. It is concluded that the present data and the explanation presented in this article are consistent with these results, and can therefore be taken as additional evidence for the spatial correlation between structural and electrical defects in *a*-Si: It appears that dangling bonds are associated with vacancy-type defects.

V. CONCLUSIONS

In summary, we have studied structural and electrical defects in amorphous Si by positron annihilation spectroscopy employing slow, variable energy positrons, and by lifetime measurements of optically generated free carriers. By making some bold assumptions on the behavior of positrons in *a*-Si (namely that the positron diffusivity and the trapping rate of vacancy-type defects in *a*-Si are equal to those in *c*-Si), an estimate for the density of vacancy-type defects in *a*-Si, prepared by ion implantation can be obtained. This density would be about 1.2 at. %, and it reduces to 0.4 at. % upon annealing at 500 °C. These values are in good agreement with several recent results based on entirely different observations, and may therefore serve as a justification for the assumptions mentioned above.

Concurrent with the apparent removal of vacancy-type defects from *a*-Si by the annealing, a tenfold increase in the lifetime of an optically generated free-carrier plasma is observed, suggesting a significant reduction in the number of band-gap states (e.g., dangling bonds). A large increase in the free-carrier lifetime has also been obtained by a low-temperature (150 °C) anneal, but with hydrogen co-implanted in the *a*-Si. Such a low temperature anneal (with co-implanted hydrogen) also leads to a reduction of the *S* parameter for positron annihilation similar to that obtained by a high-temperature anneal without hydrogen. This suggests that the band-gap states acting as trapping and recombination centers for free carriers are associated with the vacancy-type defects.

Finally, it has been found that both positron spectroscopy and carrier lifetime measurements can be a sensitive probe of ion radiation damage in 500 °C annealed *a*-Si. When the estimated density of displaced atoms due to nuclear collisions approaches 10^{-3}, both methods clearly detect a change. This suggests that the defect density in *a*-Si annealed at 500 °C is not much higher than 0.1 at. %. Moreover, at an ion damage level of several at. %, the damage saturates according to PAS, yielding independent confirmation of the estimated defect density in as-implanted *a*-Si.

ACKNOWLEDGMENTS

We gratefully acknowledge L. Venema and D. O. Boerma (Rijks Universiteit Groningen) for the low-energy H implantation and P. J. Schultz (University of Western Ontario) for comments. Work at FOM was financially supported by the Nederlandse Organisatie voor Wetenschappelijk Onderzoek (NWO) and the Stichting Technische Wetenschappen (STW).

[1] P. A. Thomas, M. H. Brodsky, D. Kaplan, and D. Lepine, Phys. Rev. B **18**, 3059 (1978).
[2] D. Turnbull, in *Beam-Solid Interactions and Phase Transformations*, edited by H. Kurz, G. L. Olson, and J. M. Poate (Materials Research Society, Pittsburgh, 1986), p. 71.
[3] S. Roorda, J. M. Poate, D. C. Jacobson, D. J. Eaglesham, B. S. Dennis, S. Dierker, W. C. Sinke, and F. Spaepen, Solid State Commun. **75**, 197(1990).
[4] S. Roorda, J. M. Poate, D. C. Jacobson, B. S. Dennis, S. Dierker, and W. C. Sinke, Appl. Phys. Lett. **56**, 2097 (1990).
[5] A. Polman, D. C. Jacobson, S. Coffa, J. M. Poate, S. Roorda, and W. C. Sinke, Appl. Phys. Lett. **57**, 1230 (1990).
[6] S. Coffa, J. M. Poate, D. C. Jacobson, and A. Polman, Appl. Phys. Lett. **58**, 2916 (1991).
[7] S. Roorda, W. C. Sinke, J. M. Poate, D. C. Jacobson, S. Dierker, B. S. Dennis, D. J. Eaglesham, F. Spaepen, and P. Fuoss, Phys. Rev. B **44**, 3702 (1991).
[8] G. N. van den Hoven, Z. N. Liang, L. Niesen, and J. S. Custer, Phys. Rev. Lett. **68**, 3714 (1992).
[9] P. J. Schultz and K. G. Lynn, Rev. Mod. Phys. **60**, 701 (1988).
[10] S. Dannefaer, P. Mascher, and D. Kerr, Phys. Rev. Lett. **56**, 2195 (1986).
[11] S. Mäkinen, H. Rajainmäki, and S. Linderoth, Phys. Rev. B **40**, 5510 (1991).
[12] P. J. Simpson, M. Vos, I. V. Mitchell, C. Wu, and P. J. Schultz, Phys. Rev. B **44**, 12180 (1991).
[13] P. Mascher, S. Dannefaer, and D. Kerr, Phys. Rev. B **40**, 11764 (1989).
[14] S. Dannefaer, D. Kerr, and B. G. Hogg, J. Appl. Phys. **54**, 155 (1983).
[15] Y. H. He, M. Hasegawa, R. Lee, S. Berko, D. Adler, and A. L. Jung, Phys. Rev. B **33**, 5924 (1986).
[16] V. G. Bhide, R. O. Dusane, S. V. Rajarshi, A. D. Shaligram, and S. K. David, J. Appl. Phys. **62**, 108 (1987).
[17] S. Coffa and J. M. Poate, Appl. Phys. Lett. **59**, 2296 (1991).
[18] J. C. Bean and J. M. Poate, Appl. Phys. Lett. **36**, 59 (1980).
[19] S. Saitoh, T. Sugii, H. Ishiwara, and S. Furukawa, Jpn. J. Appl. Phys. **20**, L130 (1981).
[20] R. A. Hakvoort, S. Roorda, A. van Veen, M. J. vanden Boogaard, F. J. M. Buters, and H. Schut, Proceedings ICPA-9 (1991).
[21] A. van Veen, J. Trace Microprobe Technol. **8**, 1 (1990).
[22] H. Schut, thesis, Delft Technical University, 1990.
[23] A. van Veen, H. Schut, J. de Vries, R. A. Hakvoort, and M. R. IJpma, in *Slow Positron Beams for Solids and Surfaces*, edited by P. J. Schultz, G. R. Massoumi, and P. J. Simpson (American Institute of Physics, New York, 1990), p. 171.
[24] R. L. Fork, B. I. Greene, and C. V. Shank, Appl. Phys. Lett. **38**, 671 (1981).
[25] P. A. Stolk, S. Roorda, L. Calcagnile, W. C. Sinke, H. B. van Linden van den Heuvell, and F. W. Saris, in *Kinetics of Phase Transformations*, edited by M. O. Thompson, M. Aziz, and G. B. Stephenson (Materials Research Society, Pittsburgh, 1992), Vol. 205, p. 15.
[26] P. A. Stolk, L. Calcagnile, S. Roorda, W. C. Sinke, A. J. M. Berntsen, and W. F. van der Weg, Appl. Phys. Lett. **60**, 1688 (1992).
[27] B. Nielsen, K. G. Lynn, A. Vehanen, and P. Schultz, Phys. Rev. B **32**, 2296 (1985).
[28] P. J. Schultz, E. Tandberg, K. G. Lynn, B. Nielsen, T. E. Jackman, M. W. Denhoff, and G. C. Aers, Phys. Rev. Lett. **61**, 187 (1988).
[29] P. Hautojärvi, P. Huttunen, J. Mäkinen, E. Punka, and A. Vehanen, Mater. Res. Soc. Symp. Proc. **104**, 105 (1988).
[30] B. Nielsen, presented at Ion Beam Modification of Materials, Knoxville, TN, 1990 (unpublished).
[31] R. B. Iverson and R. Reif, J. Appl. Phys. **62**, 1675 (1987).
[32] G. L. Olson and J. A. Roth. Mater. Sci. Rep. **3**, 1 (1988).
[33] TRIM: J. F. Ziegler, J. P. Biersack and U. Littmark, *The Stopping and Range of Ions in Solids* (Pergamon, New York, 1985), the version 1989 was used; the estimated number of displaced target atoms per ion may vary by a factor of 2 depending on which version has been used.
[34] A. Esser, K. Siebert, H. Kurtz, G. N. Parsons, C. Wang, B. N. Davidson, G. Lucovsky, and R. J. Nemanich, Phys. Rev. B **41**, 2879 (1990).
[35] M. C. Downer and C. V. Shank, Phys. Rev. Lett. **56**, 761 (1986).
[36] W. Rehm and R. Fischer, Phys. Status Solidi B **94**, 595 (1979).
[37] P. A. Stolk (unpublished).
[38] J. S. Custer, M. O. Thompson, D. C. Jacobson, J. M. Poate, S. Roorda, W. C. Sinke, and F. Spaepen, in *Beam-Solid Interactions: Physical Phenomena*, edited by J. A. Knapp, P. Borgesen, and R. A. Zuhr (Materials Research Society, Pittsburgh, 1990), Vol. 157, p. 689.
[39] C. A. Volkert and A. Polman, in *Phase Formation and Modification by Beam-Solid Interaction*, edited by G. S.Was, L. E. Rehn, and D. M. Follsteadt (Materials Research Society, Pittsburgh, 1992), Vol. 235, p. 3.
[40] M. J. Puska, C. Corbel, and R. M. Nieminen, Phys. Rev. B **41**, 9980 (1990).
[41] G. Dlubek and R. Krause, Phys. Status Solidi A **102**, 443 (1987).
[42] Motoko-Kwete, D. Segers, M. Dorikens, L. Dorikens-Vanpraet, P. Clauws, and I. Lemahieu, in *Proceedings of the 8th International Conference on Positron Annihilation*, edited by L. Dorikens-Vanpraet, M. Dorikens, and D. Segers (World Scientific, Singapore, 1989), p. 687.
[43] M. Shimotamai, Y. Ohgino, H. Fukushima, Y. Nagayasu, T. Mihara, K. Inoue, and M. Doyama, Inst. Phys. Conf. Ser. **59**, 241 (1981).
[44] K. F. Heidemann, M. Grüner, and E. te Kaat, Radiat. Effects **82**, 103 (1984).